IEEE Photonics Journal
An IEEE Photonics Society Publication

Open Access

Flexible Baseband-Unit Aggregation Enabled by Reconfigurable Multi-IF Over WDM Fronthaul

Volume 10, Number 1, February 2018

Haiyun Xin
Hao He
Kuo Zhang
Syed Baqar Hussain
Weisheng Hu

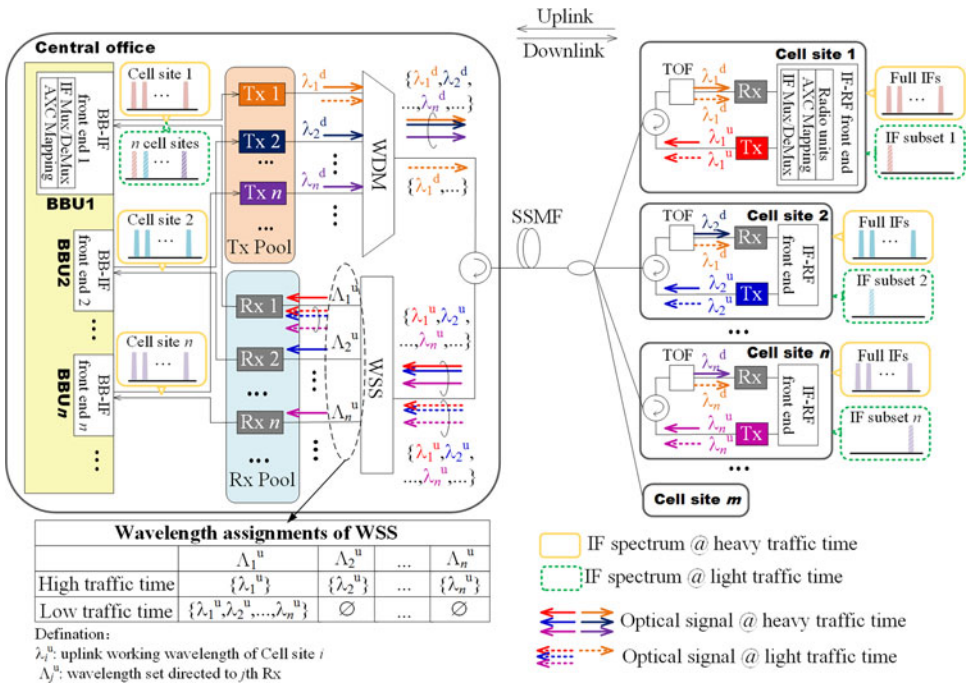

DOI: 10.1109/JPHOT.2017.2780090

Flexible Baseband-Unit Aggregation Enabled by Reconfigurable Multi-IF Over WDM Fronthaul

Haiyun Xin, Hao He, Kuo Zhang, Syed Baqar Hussain, and Weisheng Hu

State Key Laboratory of Advanced Optical Communication Systems and Networks, Shanghai Jiao Tong University, Shanghai 200240, China

DOI:10.1109/JPHOT.2017.2780090

Manuscript received August 20, 2017; revised November 7, 2017; accepted November 30, 2017. Date of publication December 11, 2017; date of current version January 3, 2018. This work was supported in part by the National Science and Technology Major Project of the Ministry of Science and Technology of China (2015ZX03001021) and in part by the National Natural Science Foundation of China (61431009, 61371082, and 61521062). Corresponding author: Weisheng Hu (email: wshu@sjtu.edu.cn).

Abstract: In cloud-radio access network, baseband-unit (BBU) aggregation schemes have been intensively discussed to improve the efficiency of resources in light traffic times. Also, driven by the emerging optical fronthaul, traffic migration is introduced in optical fronthaul to help realize BBU aggregation, based on which traffic exchange within BBU pool can be reduced, thus decreasing corresponding processing latency and energy consumption. However, these traffic migration schemes are operated in a time-division multiplexing way and are not suitable for multi-IF over wavelength-division multiplexing (WDM) fronthaul. In this paper, we propose a reconfigurable multi-IF over WDM fronthaul to support BBU aggregation. Based on IF traffic migration and optical path reconfiguration, traffic of multiple cell sites can be routed to one BBU to achieve BBU aggregation. Proof-of-concept experiments are demonstrated to verify the feasibility of the proposed architecture. For 4G+ deployment as specified in 3GPP protocol, 100-MHz orthogonal frequency-division multiplexing signal with 64 quadratic-amplitude modulation format after transmission shows that 3.5% error vector magnitude can be achieved.

Index Terms: Baseband unit aggregation, multi-IF over WDM fronthaul, optical path reconfiguration.

1. Introduction

Considering both swiftly growing mobile traffic and requirements of green infrastructure in 5G mobile communication, cloud-radio access network (C-RAN) has been widely regarded as a promising solution [1]. The baseband units (BBUs) are partitioned from conventional base stations, and pooled in central office side, leaving simple remote radio units (RRUs) as access points (APs) to the user terminals. With this BBU pooling, resources can be statistically multiplexed and power consumption can be reduced. In particular, when traffic is light, the BBU will be inefficiently utilized. In this case, traffic from multiple BBUs can be migrated to one BBU in order to reduce the working number of BBUs and save energy, which is termed as BBU aggregation [2]. However, as Fig. 1(a) shows, to realize BBU aggregation, a mass of data and signaling need to be exchanged among BBUs, which increases processing latency and power consumption [2]. Therefore, it is beneficial to introduce traffic migration function in the optical layer, which can help to reduce data exchange in BBU pool [3].

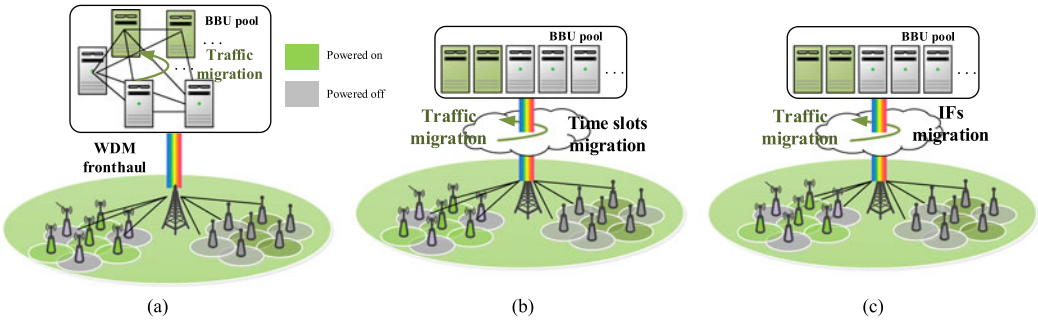

Fig. 1. (a) Traffic migration within BBU pool. (b) Traffic migration by time slots migration in digital fronthaul. (c) Proposed traffic migration by IFs migration in multi-IF based analog fronthaul.

Previously, traffic migration in optical fronthaul has been an attractive research area, which is usually based on changing the connection between BBUs and cell sites. In [4], wavelength switch and time slot switch are operated before BBU pool. In [5], cell site can be registered onto arbitrary wavelength, and its master BBU extracts the corresponding time slots. With the common time division multiplexing (TDM) feature, these schemes can be collectively labeled as time slots migration as shown in Fig. 1(b). However, these schemes are for digital interface, the common public radio interface (CPRI) [6], whose capacity is limited due to the bandwidth inefficiency. For bandwidth-efficient analog interface, traffic migration has not been considered [7]–[9]. Multi-IF over WDM is one of the most important analog interface solutions, and has been widely studied. A cell site's multiple antenna-carriers (AxCs) are converted to different IFs and then combined together. Thereafter, each cell site uses a pair of wavelengths for the bidirectional transmission of the combined IF signals. Previously, most of the studies focus on its physical performance and are demonstrated in a point-to-point scenario [7]–[9]. However, none have discussed how to support flexible connection between BBUs and cell sites, which can favor IF traffic migration, as shown in Fig. 1(c).

In this paper, in order to achieve IF traffic migration, we propose a reconfigurable multi-IF over WDM fronthaul supporting flexible connection between BBUs and cell sites. To the best of our knowledge, it is the first paradigm of flexible BBU aggregation based on multi-IF over WDM fronthaul. During heavy traffic times, the WDM fronthaul is configured as a point-to-point topology, which makes each BBU dedicatedly process one cell site in conventional way. During light traffic times, the IF traffic of multiple cell sites can be migrated to a common BBU to achieve aggregation. The operation is realized by IF traffic migration and optical path reconfiguration. One significant novelty of this work is that, for many-to-one uplink connection, parallel signal detection (PSD) is adopted [10]. Compared with other many-to-one uplink schemes [11], [12], the PSD scheme shows superiority in terms of performance and is compatible with low-cost intensity modulation direct detection (IM-DD) system. By experiments, the feasibility of the proposed scheme is validated. For 4G+ deployment specified in 3GPP specifications [13], 100 MHz OFDM signal of 64 QAM format after transmission shows that 3.5% EVM can be achieved.

2. Operation Principles

In this section, working principle of the proposed architecture is introduced. In section 2.1, we first illustrate the connection between BBUs and cell sites in different traffic times. Then, based on it, we show the supporting architecture and the configuring procedures in Section 2.2.

2.1 Connection Illustration in Different Traffic Times

During heavy traffic times, all the AxCs in cell site side are active and the traffic of each cell site occupies full IFs. Each cell site is connected to its own BBU with a pair of wavelengths for downlink

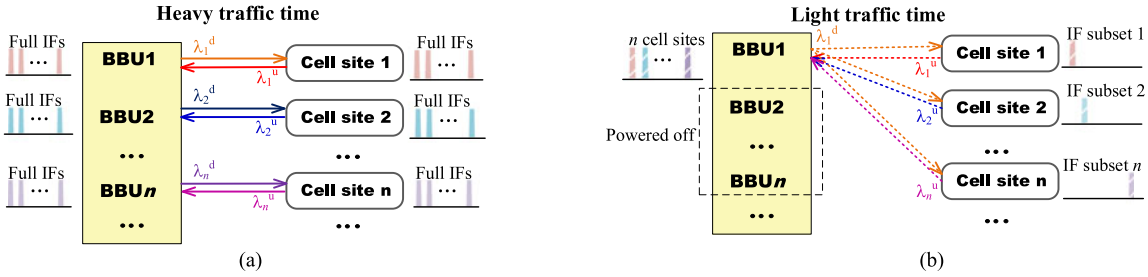

Fig. 2. Connection illustration in: (a) Heavy traffic times, (b) light traffic times. Different colors indicate different wavelengths.

and uplink, as shown in Fig. 2(a). During light traffic times, each cell site occupies a reduced number of IFs due to switching off AxCs [14]–[16], and traffic of multiple cell sites are migrated into one BBU to achieve BBU aggregation, as shown in Fig. 2(b). These cell sites are assigned with non-overlapped IFs to avoid collision. Then optical path is configured accordingly. In downlink direction, a common wavelength ($\lambda_1{}^{\mathrm{d}}$) is distributed to a group of cell sites and each cell site extracts its own IFs. In uplink direction, IF subsets from multiple cell sites, carried by respective wavelengths, are routed to a common receiver for simultaneous detection. These aggregated IFs are then processed by a common BBU. In the example of Fig. 2(b), BBU_1 is assumed as the aggregated one, which serves the group consisting Cell site 1 $\sim$ *n;* while other BBUs are powered off. IF subsets of Cell site 1 $\sim$ *n* are respectively noted as IF subset 1, IF subset 2, . . . , IF subset *n*.

It is worthwhile to mention that, for many-to-one uplink transmission in light traffic time, multiple wavelengths are simultaneously detected, which is termed as PSD. It is based on the law that, a common receiver is able to simultaneously detect optical signals from multiple sources as long as the wavelength frequency difference of any two wavelengths is beyond the bandwidth of photodetector (PD), and the detailed principles are illustrated in the appendix. The following benefits can be obtained from this method: (i) It is able to avoid signal impairments induced by beat noise, compared with detecting multiple signals of same wavelength in [11]. (ii) It is compatible with conventional IM-DD infrastructure, since extra signal processing techniques are not required to remove the interference caused by incoherence of different lasers [12].

2.2 The Supporting Architecture

Fig. 3 shows the intact architecture which supports the aforementioned two kinds of connection in section 2.1, and the detailed operation procedures. Besides, IF and wavelength assignments in different traffic situations are marked at the proper locations. The configuration for downlink transmission is by tuning optical filter in cell site side. In the example, tunable optical filters (TOFs) in Cell site 1 $\sim$ *n* are respectively tuned at $\lambda_1{}^{\mathrm{d}}$, $\lambda_2{}^{\mathrm{d}}$, $\lambda_3{}^{\mathrm{d}}$, . . . , $\lambda_n{}^{\mathrm{d}}$ in heavy traffic times, and all are tuned at $\lambda_1{}^{\mathrm{d}}$ in light traffic times. For uplink, the configuration is operated with WSS. The wavelength assignments are listed in the left bottom table shown in Fig. 3. $\Lambda_j{}^{\mathrm{u}}$ denotes the wavelength set directed to receiver *j*. During heavy traffic times, the WSS is configured to route one wavelength to each receiver, just acting as a wavelength de-multiplexer (DeMux). $\Lambda_j{}^{\mathrm{u}}$ contains only one uplink wavelength in this case. And during light traffic times, the uplink wavelengths are divided into different sub-sets and each is detected by one corresponding receiver of aggregated BBU, whereas receivers of other BBUs will be off and receive no wavelength from WSS. In the example, BBU_1 is the aggregated one, where $\Lambda_1{}^{\mathrm{u}} = \{\lambda_1{}^{\mathrm{u}}, \lambda_2{}^{\mathrm{u}}, \ldots, \lambda_n{}^{\mathrm{u}}\}$, and $\Lambda_2{}^{\mathrm{u}} \ldots, \Lambda_n{}^{\mathrm{u}} = \emptyset$.

3. Transmission Performance

To evaluate transmission performance, the proposed scheme is experimentally demonstrated. The radio signal is selected in accordance with 4G+ deployment as specified in 3GPP. To obtain high

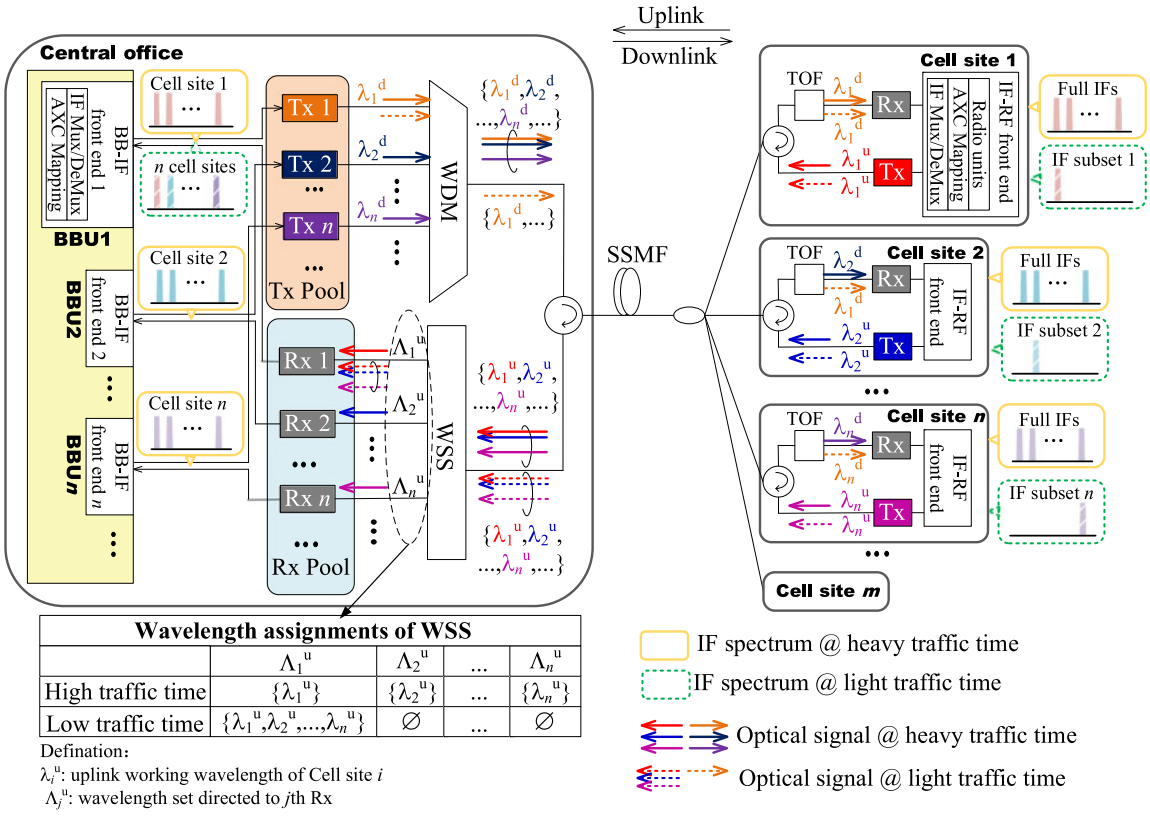

Fig. 3. Proposed reconfigurable multi-IF over WDM fronthaul architecture. BBU: baseband unit, AxC: Antenna-carrier, WSS: wavelength selective switch, WDM: wavelength division multiplexing, IF: intermediate frequency, TOF: tunable optical filter. In heavy traffic times, each BBU dedicatedly serves one cell site. In light traffic times, BBU_1 simultaneously serves n cell sites, while $BBU_2 \sim BBU_n$ are powered off.

bandwidth efficiency, we choose the scheme described in [10], where contiguous carrier aggregation is adopted. We assume that a cell site with full load will occupy 12 IFs in single direction, each of which is a 100 MHz 64 QAM OFDM signal (5 $\times$ 20 MHz carrier-aggregation).They are respectively located at $i \times$ 150 MHz, where $i = 1, 2, \ldots, 12$, with 50 MHz guard bands between two adjacent IFs. Corresponding CPRI-equivalent data rate is about 75Gbps. We demonstrate a system with 4 cell sites, for downlink and uplink respectively, and emulate three traffic situations: (i) heavy traffic scenario where no BBU is aggregated and each is connected to only one cell site, which occupies all the12 IFs; (ii) moderate traffic scenario where the aggregated BBU is connected to two cell sites, each of which occupies 6 IFs and (iii) light traffic scenario where the aggregated BBU is connected to all the four cell sites, each of which occupies 3 IFs.

3.1 Downlink Transmission

According to the downlink principles in section 2.1, the receiver detects all the 12 IFs in either scenario. The distinction for different traffic situations is reflected through how many IFs are extracted in the cell site side. Thus, for simplicity, the experiment illustrated in Fig. 4 is used to emulate all the three scenarios mentioned above. In CO, the continuous optical wave from a DFB laser (launch power: 7 dBm) followed by a polarization controller (PC) is injected to a Mach-Zehnder Modulator (MZM) biased at the quadrature point. This MZM is driven by amplified combined 12 IFs, which emulates traffic for one or multiple cell sites. The modulation depth is optimized, with an optical modulation index (OMI) of 0.14, which is calculated according to the definition in [17]. Signal

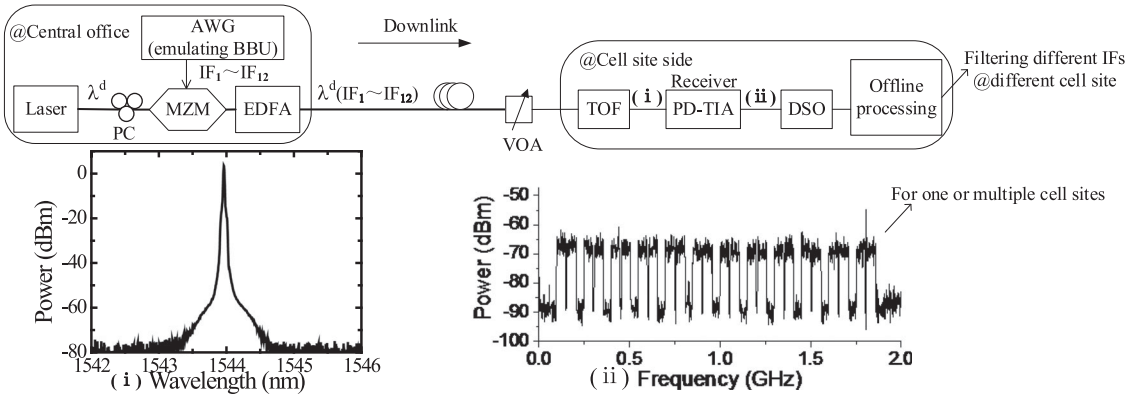

Fig. 4. Experimental setup of downlink transmission. Optical and electrical spectrum at selected locations. PC: polarization controller. MZM: Mach-Zehnder Modulator. EDFA: erbium doped fiber amplifier VOA: variable optical attenuator. PD: photodetector. TIA: Trans-impedance amplifier. DSO: digital storage oscilloscope. (i) Optical spectrum before receiver. (ii) Electrical spectrum after PD detection.

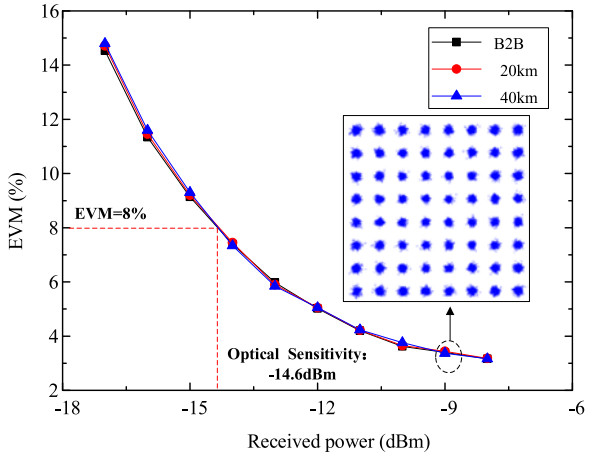

Fig. 5. Average EVM of received OFDM signal vs received power.

generation is implemented by an arbitrary waveform generator (AWG) with the sampling rate of 10 GSa/s. The output power of MZM is 1 dBm and then boosted by an EDFA to 11 dBm and launched into a standard single mode fiber (SSMF). At cell site side, a variable optical attenuator (VOA) serves as the splitter loss. Then the optical signal filtered with a TOF is retrieved by a PD-TIA with a 3 dB bandwidth of 3 GHz, which emulates the receiver. And it is sent to a digital sampling oscilloscope (DSO) at 10 GSa/s for digitization and offline processing. Offline procedures include manual timing synchronization, appropriate IF filtering, frequency down conversion, and OFDM demodulation. The optical spectrum after TOF and the electrical spectrum after PD-TIA are inserted in Fig. 4.

The experimental results are illustrated in Fig. 5, where average error vector magnitude (EVM) of 12 IFs after transmitting 0 km, 20 km and 40 km are shown. EVM of 3.5% can be achieved at −8 dBm. When the received power gets small, the EVM performance degrades due to thermal noise. 8% EVM (Maximum allowable EVM for 64-QAM OFDM signal specified in 3 GPP standard [12]) is achieved at −14.6 dBm received power. Considering the insertion loss of WDM (2 dB), and TOF (2 dB), the power budget is 22 dB. The dispersion penalty is negligible, because total bandwidth is only less than 2 GHz.

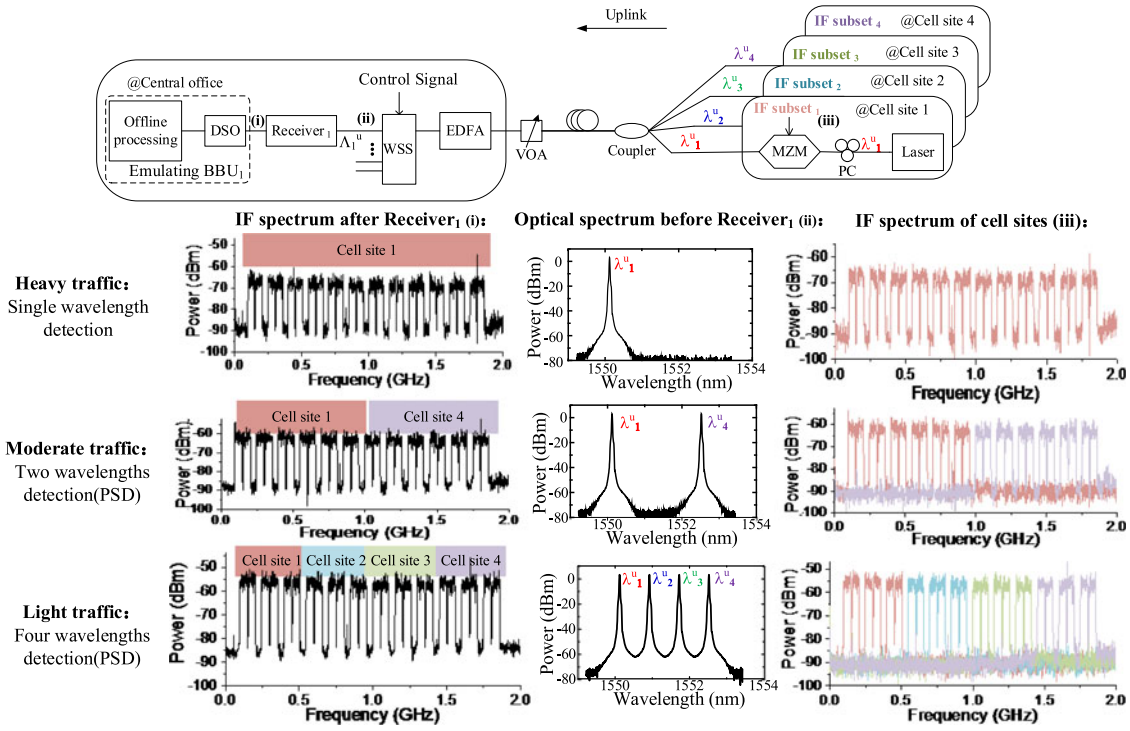

Fig. 6. Experimental setup of uplink transmission. WSS: wavelength selective switch. (i) Electrical spectrum after Receiver$_1$ @ different traffic times; (ii) Optical spectrum of signal routed Receiver$_1$ @ different traffic times; (iii) Electrical spectra of related cell sites @ different traffic times.

TABLE 1
IF Subsets Assignments

	Cell site 1	Cell site 2	Cell site 3	Cell site 4
Heavy traffic	IF 1 ∼ 12	IF 1 ∼ 12	IF 1 ∼ 12	IF 1 ∼ 12
Moderate traffic	IF 1 ∼ 6	IF 1 ∼ 12	IF 1 ∼ 12	IF 7 ∼ 12
Light traffic	IF 1 ∼ 3	IF 4 ∼ 6	IF 7 ∼ 8	IF 10 ∼ 12

3.2 Uplink Transmission

The experimental setup for uplink transmission is depicted in Fig. 6. Unlike downlink, experimental procedure of uplink varies for different traffic situations. First, IF signals are generated according to the IF assignments shown in Table 1. To imitate multiple cell sites in moderate and light traffic scenarios, multiple independent AWG channels are used. Uplink wavelengths are fixed as $\lambda_1^u = 1550.12\,\text{nm}$, $\lambda_2^u = 1550.92\,\text{nm}$, $\lambda_3^u = 1551.72\,\text{nm}$, and $\lambda_4^u = 1552.52\,\text{nm}$ for Cell site 1 ∼ 4 respectively. After the coupled four wavelengths reaching central office, WSS is configured to allocate wavelength to receivers, according to Table 2. For simplicity, analysis for all traffic cases is conducted only for corresponding receiver of BBU$_1$, which is named as Receiver$_1$. During heavy traffic times, it is assumed that every cell site is running at heavy load and WSS will allocate only λ_1^u to Receiver$_1$. During moderate traffic times, it is assumed that Cell site 1 and Cell site 4 are running at moderate load and Cell site 2 and Cell site 3 are running at heavy load. So λ_1^u and λ_4^u

TABLE 2
Wavelength Allocation in Different Traffic Times

	Λ_1^u	Λ_2^u	Λ_3^u	Λ_4^u
Heavy traffic	$\{\lambda_1^u\}$	$\{\lambda_2^u\}$	$\{\lambda_3^u\}$	$\{\lambda_4^u\}$
Moderate traffic	$\{\lambda_1^u, \lambda_4^u\}$	$\{\lambda_2^u\}$	$\{\lambda_3^u\}$	$\emptyset$
Light traffic	$\{\lambda_1^u, \lambda_2^u, \lambda_3^u, \lambda_4^u\}$	$\emptyset$	$\emptyset$	$\emptyset$

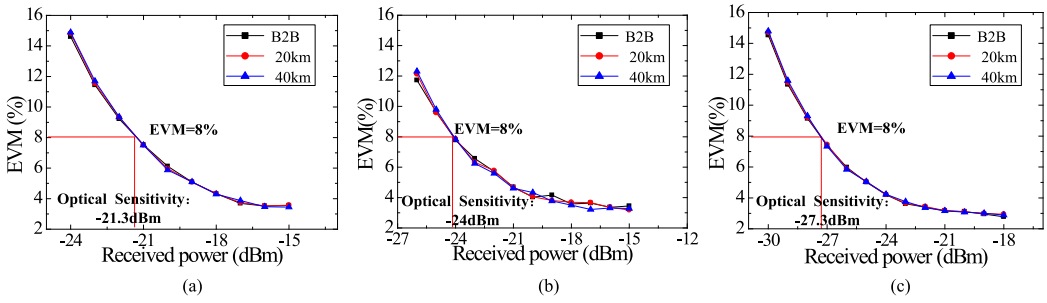

Fig. 7. Average EVM of received OFDM signal vs received power of each wavelength. (a) Heavy traffic times. (b) Moderate traffic times. (c) Light traffic times.

are aggregated in Receiver$_1$. During light traffic times, it is assumed that, all cell sites are running at light load and λ_1^u, λ_2^u, λ_3^u and λ_4^u are all aggregated in Receiver$_1$. The optical spectrum before Receiver$_1$ and electrical spectrum after Receiver$_1$ at different traffic times are inserted in Fig. 6. The background colors indicate the IFs come from which cell site.

During heavy traffic times, EVM versus received power (measured before EDFA) is illustrated in Fig. 7(a). It is found that, 8% EVM is achieved at -21.2 dBm regardless of the fiber length so almost no dispersion penalty is observed. Considering the launched power (1 dBm) and insertion loss of WSS (4.5 dB), about 18 dB power budget is achieved. During moderate traffic times, PSD is implemented. Since wavelength spacing is far larger than the cut-off frequency of PD (3 GHz), no beat noise occurs, which can be seen from the electrical spectrum after Receiver$_1$. Here, each wavelength has same launched and same received power. The performance of each IF is almost same and only average EVM of 12 IFs is shown in Fig. 7(b). 8% EVM is achieved at -24 dBm received power per wavelength. As a consequence, 21 dB power budget is achieved. During light traffic times, the average EVM performance of 12 IFs is shown in Fig. 7(c). 8% EVM condition is satisfied at -27.2 dBm per wavelength, and 24 dB power budget is achieved. Comparing experimental results of the three scenarios, the sensitivity increases by nearly 3 dB, when the number of detected wavelengths increases twice. It is because that, when each cell site transmits half the number of IFs, each IF obtains twice electrical gain before driving optical modulator.

It is found that the lower bound of average EVM performance (3.5%@ heavy traffic times, 3.2%@ moderate traffic times, 2.9%@ light traffic times) gets better when number of detected wavelengths increases. There are mainly two reasons for this. Firstly, effective number of bits (ENOB) increase when AWG generates less IFs [18]. In the experiment of heavy traffic times, the AWG outputs 12 IFs, and in experiments of moderate traffic times and light traffic times each AWG outputs 6 IFs and 3 IFs respectively. Secondly, the main nonlinear effects are due to limited linear zone of modulation curve of MZM and power-current curve of PD [9], [19], [20]. Both of the nonlinearities occur within each wavelength channel. For modulation, different IF subsets are independently converted to optical signal. For detection, the interaction between different wavelengths is filtered out by the

limited bandwidth of PD. The harmonics and intermodulation products occur among the IFs within a common wavelength channel, and the amount of these products is positively correlated to the IF number. Thus, more IFs of single wavelength will induce more severe nonlinear effect. Overall, PSD can even bring slight improvement in signal performance.

3.3 Summary of Experiments

In the above experiments, we have demonstrated that our scheme is capable of traffic migration in the optical layer to realize BBU aggregation. In a practical deployment, the flexiblility degree and the cost might be two major concerns. (i) Though flexibility for BBU aggregation is verified by the experiments in the case with four cell sites and three traffic times, any other cases should also be supported since the WSS can fulfill completely flexible wavelength allocation. (ii) The adoption of PSD in uplink enables the implementation of low-cost IM-DD system since it can avoid performance degradation induced by detecting multiple signals with same wavelength [11], [12]. Though it is demonstrated with MZMs due to the limit of lab equipment condition, we expect intensity modulation transmitters with lower cost such as EMLs and DMLs can also be applied. Besides, according to the power budget (22 dB in downlink and 18 dB in uplink), maximum number of served cell sites is 32, 16 and 8 for 0 km, 20 km and 40 km cases respectively. Thus, cost of WSS as well as other devices at the BBU side, can be shared by all users.

4. Conclusion

In this paper, we propose a reconfigurable multi-IF over WDM fronthaul, which can support flexible BBU aggregation. The connection between BBUs and cell sites can be adjusted according to the time varying traffic demands. Thus, BBU aggregation can be achieved by traffic migration in optical layer, reducing a mass of data exchange within BBU pool. The operation is realized by IF migration and optical path reconfiguration. In particular, with the adoption of PSD in uplink, the low-cost IM-DD system can be utilized and no performance degradation is caused. Proof-of-concept experiments are demonstrated in 4G+ deployment as specified in 3GPP protocol. 100 MHz 64 QAM format OFDM signal after 40 km transmission shows that, 3.5% EVM can be achieved. Therefore, the proposed scheme can well support the BBU aggregation, which caters to the goals of next generation communication network.

Appendix

Theory Principle of PSD

In this part, we demonstrate that the output signal of PSD is simply the composite of output of multiple direct detection. Fig. 8 shows the block diagram of PSD. Signal process among modulator, adder and detector is described. Assume that two input electrical domain signals are respectively written as a_1 (t) and a_2 (t), noting they occupy collision-free frequency spectrum and modulate two light waves at λ_1 and λ_2, thus the corresponding optical field signals are described as:

$$r_1(t) = (1 + M_1 a_1(t)) \times \cos(2\pi f_{\lambda_1} t) \tag{1}$$

$$r_2(t) = (1 + M_2 a_2(t)) \times \cos(2\pi f_{\lambda_2} t) \tag{2}$$

where f_{λ_1} and f_{λ_2} denote the frequencies of optical carriers, and M_1 and M_2 denote the modulation depths. The output of optical adder is written as

$$r(t) = (1 + M_1 a_1(t)) \times \cos(2\pi f_{\lambda_1} t) + (1 + M_2 a_2(t)) \times \cos(2\pi f_{\lambda_2} t) \tag{3}$$

Due to noncoherent detection, the receiver acts as an envelope detector where the output electrical domain signal is determined by the power intensity of input optical signal. Therefore, the receiver is equivalent to a two stage system which contains a square-law detector and a low pass

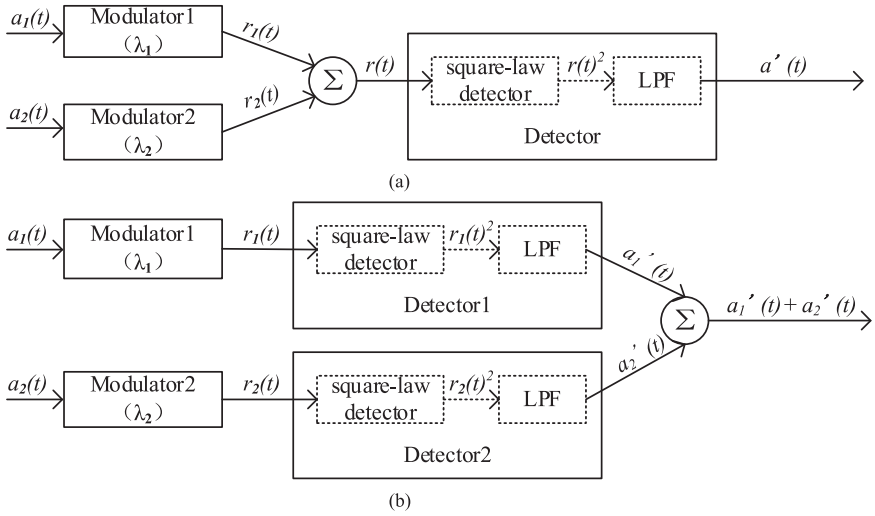

Fig. 8. (a) Block diagram of parallel signal detection. (b) Equivalent block diagram of parallel signal detection.

filter (LPF) with the cut-off frequency same as the PD's working bandwidth. The output of square-law detector is $r(t)^2$, which is consisted of a cross-term $2r_1(t) \times r_2(t)$ and two quadratic-terms $r_1(t)^2$, $r_2(t)^2$.

The cross-term contains two frequency components: $f_{\lambda_1} + f_{\lambda_2}$ and $|f_{\lambda_1} - f_{\lambda_2}|$. Obviously, $f_{\lambda_1} + f_{\lambda_2}$ is far higher than the cut-off frequency of LPF, and will be eliminated, so we only need to pay attention to $|f_{\lambda_1} - f_{\lambda_2}|$. When $|f_{\lambda_1} - f_{\lambda_2}|$is lower than the cutoff frequency, the corresponding frequency component will pass the filter, resulting in beat-photocurrent signals, which may occupy the frequency spectrum of useful signal. On contrary, when $|f_{\lambda_1} - f_{\lambda_2}|$ is higher than the cutoff frequency of low pass filter, the corresponding component will be eliminated, which means only the two quadratic-terms need to be considered.

Hence, the two wavelengths can be parallelly detected provided that the frequency difference between two wavelengths is larger than the working bandwidth of PD. As is shown in Fig. 8(b), the output signal of PD is:

$$a'(t) = a'_1(t) + a'_2(t) \tag{4}$$

where $a'(t)$ denotes realistic output signal,$a'_1(t)$ and $a'_2(t)$ respectively denote the output signal of only detecting λ_1 or λ_2. Obviously, $a'_1(t)$ and $a'_2(t)$ remain collision-free. Similarly, when the received number is n, the frequency difference should be satisfied between any two wavelengths, and the output signal is the composite of n wavelengths. Although PD is shared, the whole optical link works as an IM-DD system for each wavelength channel.

In our proposed architecture, WSS works as an adder when routing multiple wavelengths to a PD. The input signal $a_i(t)(i = 1, 2, 3, ..., n)$ is IF multiplexing signal from Cell site i, n is the number of cell sites sharing a receiver at the CO side. In parallel detection scenario,$a_i(t)$ occupy frequency spectrum of different range. After detected at the CO, no frequency offset occurs, the IFs remain at same frequency point as before.

References

[1] I. Chih-Lin, C. Rowell, S. Han, Z. Xu, G. Li, and Z. Pan, "Toward green and soft: A 5G perspective," *IEEE Commun. Mag.*, vol. 52, no. 2, pp. 66–73, Feb. 2014.

[2] X. Wang *et al.*, "Green virtual base station in optical-access-enabled cloud-RAN," in *Proc. IEEE Int. Conf. Commun., Opt. Netw. Syst. Symp.*, 2015, 5002–5006.

[3] W. Hu *et al.*, "Soft-stacked PON for soft C-RAN," *J. Opt. Commun. Netw.*, vol. 8, no. 11, pp. B12–B20, Nov. 2016.
[4] A. Nag, Y. Zhang, L. A. DaSilva, L. Doyle, and M. Ruffini, "Integrating wireless BBUs with optical OFDM flexible-grid transponders in a C-RAN architecture," presented at the Opt. Fiber Commun. Conf., Los Angeles, CA, USA, 2017, Paper M2G-2.
[5] J. Zhang, Y. Ji, X. Xu, H. Li, Y. Zhao, and J. Zhang, "Energy efficient baseband unit aggregation in cloud radio and optical access networks," *J. Opt. Commun. Netw.*, vol. 8, no. 11, pp. 893–901, Nov. 2016.
[6] CPRI specification V6.1 (2014-7-1). (2014) [Online]. Available: http://www.cpri.info/spec.html
[7] M. Zhu, X. Liu, N. Chand, F. Effenberger, and G. K. Chang, "High-capacity mobile fronthaul supporting LTE advanced carrier aggregation and 8× 8 MIMO," presented at the Opt. Fiber Commun. Conf., Los Angeles, CA, USA, 2015, Paper M2J-3.
[8] X. Liu, H. Zheng, N. Chand, and F. Effenberger, "Efficient mobile fronthaul via DSP-based channel aggregation," *J. Lightw. Technol*, vol. 34, no. 6, pp. 1556–1564, Mar. 2016.
[9] C. Han, S. Cho, H. Chung, and J. Lee, "Linearity improvement of directly-modulated multi-IF-over-fibre LTE-A mobile fronthaul link using shunt diode predistorter," presented at the Eur. Conf. Opt. Commun., Valencia, Spain, 2015, Paper We.4.4.4.
[10] Y. Luo *et al.*, "WDM passive optical network with parallel signal detection for video and data delivery," presented at the Opt. Fiber Commun. Conf., Anaheim, CA, USA, 2007, Paper OWS6.
[11] M. Zhu *et al.*, "Wavelength resource sharing in bidirectional optical mobile fronthaul," *J. Lightw. Technol.*, vol. 33, no. 15, pp. 3182–3188, Apr. 2015.
[12] M. Xu *et al.*, "Bidirectional fiber-wireless access technology for 5G mobile spectral aggregation and cell densification," *J. Opt. Commun. Netw*, vol. 8, no. 12, pp. 104–110, Nov. 2016.
[13] 3GPP, 3GPP TS 36.104 version 11.9.0 release 11, 2014.
[14] S. Zhang, J. Gong, S. Zhou, and Z. Niu, "How many small cells can be turned off via vertical offloading under a separation architecture," *IEEE Trans. Wireless Commun.*, vol. 14, no. 10, pp. 5440–5453, Oct. 2015.
[15] I. Macaluso, B. Cornaglia, and M. Ruffini, "Antenna, spectrum and capacity tradeoff for cloud RAN massive distributed MIMO over next generation PONs," presented at the Opt. Fiber Commun. Conf. Exhib., Los Angeles, CA, USA, 2017, Paper M2I-1.
[16] X. Gao, O. Edfors, F. Tufvesson, and E. G. Larsson, "Massive MIMO in real propagation environments: Do all antennas contribute equally?," *IEEE Trans. Wireless Commun.*, vol. 63, no. 11, pp. 3917–3928, Nov. 2015.
[17] D. R¨orich, X. Wang, M. Bernhard, and J. Speidel, "Optimal modulation index of the Mach-Zehnder modulator in a coherent optical OFDM system employing digital pre-distortion," in *Proc. 14. 2013 ITG Symp. Photon. Netw.*, 2013, pp. 1–6.
[18] W. Du, H. Xin, H. He, and W. Hu, "A resource sharing C-RAN architecture with wavelength selective switching and parallel uplink signal detection," presented at the Asia Commun. Photon. Conf., Hong Kong, 2015, Paper ASu3E.3.
[19] D. Wake, A. Nkansah, and N. J. Gomes, "Radio over fiber link design for next generation wireless systems," *J. Lightw. Technol.*, vol. 28, no. 16, pp. 2456–2464, Aug. 2010.
[20] J. Wang *et al.*, "Nonlinear inter-band subcarrier intermodulations of Multi-RAT OFDM wireless services in 5G heterogeneous mobile fronthaul networks," *J. Lightw. Technol.*, vol. 34, no. 17, pp. 4089–4103, Sep. 2016.